Numerical Modeling of Static Hysteresis Phenomena Using a Vector Extension of the Loss Surface Model

Leopold Mikula, Brahim Ramdane, Lucas Blattner Martinho, Afef Kedous-Lebouc, Gerard Meunier

Numerical modelling of static hysteresis phenomena using a vector extension of the Loss Surface model

Léopold Mikula[1,2], Brahim Ramdane[1], Lucas Blattner Martinho[2], Afef Kedous-Lebouc[1], and Gérard Meunier[1]
[1]Université Grenoble Alpes, CNRS, Grenoble INP, G2Elab. F-38000 Grenoble, France
[2]Altair Engineering France. F-38240 Meylan, France

This paper proposes a vector extension of the Loss Surface model for numerically modelling hysteretic phenomena in electromagnetic device simulations with isotropic ferromagnetic materials. The vectorization strategy is based on Mayergoyz's approach. The developed model has been implemented in the 2D finite element code. To handle the non linear problem solved with the Newton-Raphson algorithm, a suitable method is proposed for the approximation of the reluctivity tensor. Several test cases from TEAM problem 32 were investigated for validation. The results are in good agreement with measurements combining accuracy and short computation times.

***Index Terms*—Vector magnetic hysteresis modelling, Loss Surface, Finite Element Method**

I. Introduction

THE Finite Element Method (FEM) is generally used in the analysis of electromagnetic devices. In this context, the nonlinear behaviour of ferromagnetic materials is commonly represented by a scalar, one-to-one magnetization curve in the FEM procedure. The magnetic core losses are usually computed then knowing the space and time variations of the magnetic flux density and considering *a posteriori* approaches such as the Bertotti [1] or Loss Surface (LS) [2] models. However, even if the losses estimation may be accurate with these methods, it excludes hysteresis phenomena from the magnetic field computation.

Scalar hysteresis models such as the classic implementations of the Jiles-Atherton (JA)[3] and Preisach [4] models can only describe the behaviour of soft magnetic materials subjected to unidirectional fields. To account for rotating fields, such as the ones occurring in electromechanical devices, an extension of the scalar model to a vector model is needed. For instance, Bergqvist [5] and Mayergoyz [6] have proposed vector generalizations of the scalar JA and Preisach models. One of the main difficulties in these generalizations lies in the conversion of the standard b(h) models into an inverse h(b) hysteresis operator that is more adapted to FEM formulations stated in terms of the magnetic vector potential. This point has been discussed for both models in [8] and [7]. In the past, several authors have addressed the problem of incorporating hysteresis models into FEM formulations using JA [9] or Preisach [10] model.

The LS model has been developed for a long time at the G2Elab and has been proven in loss prediction in electrical machines by using it in a post processing mode in FE Simulation. Recently it has been greatly improved in terms of accuracy and robustness. It has also been extended over saturation and high frequency [11] and [12] . Moreover, the scalar LS model is by definition a h(b) model and are consequently a good candidate for vectorization and implementation in 2D FEM analysis. So, the objective is to implement the LS static and dynamic model into FEM simulation for non-oriented materials considering at a first step an isotropic and static vectorial behavior.

The vector extension of the LS model proposed in this paper uses the well-known Mayergoyz vector extension method [6]. The suitable procedure to implement this new model in 2D finite element analysis is presented. An application to 2D transient magnetic hysteresis problem resolution is described and results are discussed.

Manuscript received November 4, 2022; revised XXX XX, XXX. Corresponding author: L. Mikula (email: lmikula@altair.com).

II. Static Loss Surface scalar Model

In this work, only the static LS model is considered. In this context, the static magnetic field intensity h_{stat} is expressed as the sum of the reversible and irreversible contributions h_{anhys} and h_{comp}

$$h_{stat} = h_{anhys} + h_{comp} \tag{1}$$

h_{anhys} represents the anhysteretic field, which is assumed to be history independent. This component corresponds to the median curve of a quasi-static hysteresis loop of the saturated material. The history dependency is considered through h_{comp}, which represents the magnetic field intensity component caused by both the bending and displacement of the domain walls.

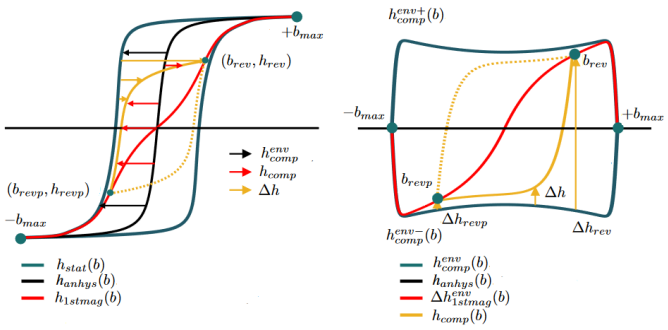

Fig. 1: Key quantities of the static LS model [11]

For any hysteresis loop, h_{comp} is defined as the difference between h_{stat} and h_{anhys}. The main purpose of the model is to estimate the value of h_{comp} in a simple way. To achieve this objective, three quantities h_{comp}^{env}, Δh and Δh_{1stmag}^{env} must be defined. The first one corresponds to the equivalent of h_{comp} for a major hysteresis loop. The second one is the difference between the static field of any hysteresis loop and the major envelope. The third one is the difference between $h_{1stmag}(b)$ and h_{anhys}. We define the first magnetization curve by the coordinates of reversal points of centred minor hysteresis loops. Equation (2) summarizes the relationships between all these quantities, which are further geometrically illustrated in Fig. 1.

$$\begin{aligned} h_{comp}^{env} &= h_{stat}^{major} - h_{anhys} \\ \Delta h &= h_{comp} - h_{comp}^{env} \\ \Delta h_{1stmag}^{env} &= h_{1stmag} - h_{anhys} \end{aligned} \tag{2}$$

As can be seen in Fig. 1, $\Delta h(b)$ decreases monotonically from the initial value Δh_{rev} to its minimum value Δh_{revp} when b varies from the reversal point b_{rev} to the previous reversal point b_{revp}. Moreover, we express the same quantities δh and δb in a relative scale as follows

$$\delta h = \frac{\Delta h - \Delta h_{revp}}{\Delta h_{rev} - \Delta h_{revp}} \text{ and } \delta b = \frac{b - b_{revp}}{b_{rev} - b_{revp}} \tag{3}$$

The decreasing behavior of δh is also ensured in the case of minor loop. In this way, all the reversal curves of a hysteresis loop have the same kind of variations even if these curves have different value of b_{rev} and b_{revp}. Thus, we can compute h_{comp} by using a unique function f which describes δh now called the unit differential reversal curve (uDRC) as described in [11].

$$\begin{aligned} h_{comp} &= (\Delta h_{rev} - \Delta h_{revp})\,\delta h + h_{comp}^{env} \\ \text{where } \delta h &= f(\Delta b_{rev}, \delta b) \end{aligned} \tag{4}$$

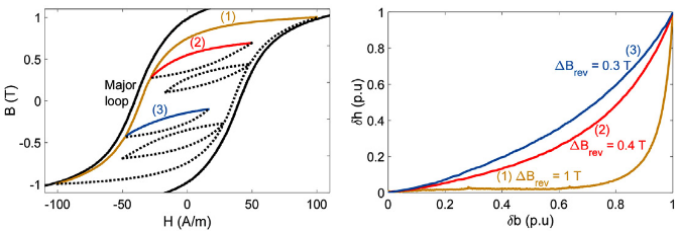

Fig. 2: uDRC principal [11]

The values of the coefficients used in the analytical functions f and h_{comp}^{env} may be obtained through the measurement of the major hysteresis loop and few centered hysteresis cycles through data-fitting. The detailed procedure employed to determine them is described in [11].

III. Isotropic Vector Model

Scalar hysteresis models are not suitable for describing the behaviour of a material subjected to rotating fields. Consequently, a vector extension of the LS model based on Mayergoyz's method is here proposed. The main idea of this method is to combine the contribution of scalar models continuously distributed in space. Vector $\boldsymbol{b}$ is projected on all directions and can be expressed in two dimensions as in (5), where $\boldsymbol{e_\phi}$ is a unit vector along the direction defined by an angle ϕ

$$\boldsymbol{b} = \int_{-\frac{\pi}{2}}^{\frac{\pi}{2}} \boldsymbol{b} \cdot \boldsymbol{e_\phi} d\phi \text{ where } \boldsymbol{e}_\phi = [\cos\phi, \sin\phi] \tag{5}$$

Then, each projected value of $\boldsymbol{b}$ on the direction ϕ is taken to be the input of the scalar model, thus each direction has its own history. Finally, $\boldsymbol{h}$ is obtain by vectorial sum of each output of the scalar models.

We choose to only project the irreversible part $\boldsymbol{h_{comp}}$, while $\boldsymbol{h_{anhys}}$, the reversible part remains co-linear to $\boldsymbol{b}$. This is physically consistent because the phase delay between $\boldsymbol{h}$ and $\boldsymbol{b}$ is due to irreversibly of the magnetization process which is estimated by h_{comp} in our model. In addition, h_{comp} tends to zero close to saturation, making $\boldsymbol{h}_{stat}$ and $\boldsymbol{b}$ parallel.The 2D, isotropic, vector LS model may then be stated as follows:

$$\boldsymbol{h_{stat}} = h_{anhys}(\|\boldsymbol{b}\|)\frac{\boldsymbol{b}}{\|\boldsymbol{b}\|} + \int_{-\frac{\pi}{2}}^{\frac{\pi}{2}} \boldsymbol{e}_\phi \cdot h_{comp}(\boldsymbol{b} \cdot \boldsymbol{e}_\phi) d\phi \tag{6}$$

In Fig.3.a), we plotted the magnetic loss evolution vs $\boldsymbol{b}$ amplitude under uniaxial and circular induction obtained by the vector LS model. The curves are compared to measurements and scalar LS model results. The model shows good results under uniaxial excitation. However, the static rotational loss remains constant and doesn't tend to zero at saturation as it has been observed experimentally [13]. Fig 3.b) shows the phase delay between $\boldsymbol{h}_{stat}$ and $\boldsymbol{b}$ obtained with rotating excitation at 10 Hz. It seems to be consistent with the measurement obtained by Matsuo [14]. The phase delay decreases significantly close to saturation but never reaches zero. As a result, non-zero rotating losses. This could be because some projection directions are not saturated. This point must be improved in a future work.

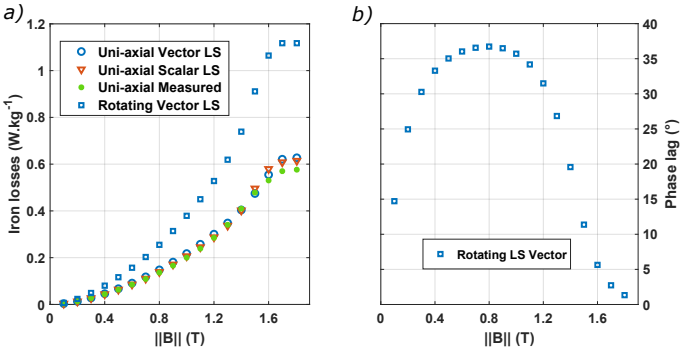

Fig. 3: a) Iron losses M40050A, at 10 Hz
b) Phase lag between $\boldsymbol{h}_{stat}$ and $\boldsymbol{b}$ for rotating field at 10 Hz

A Gauss-Legendre quadrature procedure is adopted to numerically evaluate the integral in equation (6). The number and the orientation of the unit vector $\boldsymbol{e}_\phi$ as well as w_i the weights assigned to direction i are fixed by the degree of the quadrature. For a suitable precision we consider 21 directions. The 2D, isotropic vector LS model may then be stated as follows

$$\boldsymbol{h}_{stat} = h_{anhys}(\|\boldsymbol{b}\|)\frac{\boldsymbol{b}}{\|\boldsymbol{b}\|} + \frac{2}{\pi}\sum_{i=1}^{N} \omega_i \boldsymbol{e_{\phi,i}} \cdot h_{comp}(\boldsymbol{b} \cdot \boldsymbol{e}_{\phi,i}) \tag{7}$$

IV. FEM IMPLEMENTATION

The developed model has been used for solving magnetic transient nonlinear problems neglecting eddy currents. This section outlines the FEM implementation procedure based on the 2D magnetic vector potential formulation $\boldsymbol{a}$ on a domain Ω in the plane xOy

$$\boldsymbol{b} = \boldsymbol{curla} \tag{8}$$

The weak formulation is obtained by multiplying the Ampere law equation $\boldsymbol{curlh} = \boldsymbol{j}$ by a test function $\boldsymbol{W}$ and integrating over the domain Ω. Where $\boldsymbol{h}$ is the magnetic field and $\boldsymbol{j}$ the current density. $\boldsymbol{W}$ is chosen equal to the nodal shape function and expanded in terms of vector shape functions $\boldsymbol{W_i} = (0, 0, w_i)^t$. We obtain

$$\int_\Omega \boldsymbol{curlW} \cdot \boldsymbol{h} d\Omega = \int_\Omega \boldsymbol{W} \cdot \boldsymbol{j} d\Omega \tag{9}$$

The Newton-Raphson (NR) method is applied to solve the non-linear system at each time step. This method requires to evaluate the Jacobian matrix $\boldsymbol{Jac}$ associated to (9) which can be expressed as follows

$$\boldsymbol{Jac} = \int_\Omega \boldsymbol{curlW_i} \cdot \left[\frac{\boldsymbol{\partial h}}{\boldsymbol{\partial b}}\right] \cdot \boldsymbol{curlW_j d\Omega} \tag{10}$$

Equation (10) shows the differential reluctivity tensor $\left[\frac{\boldsymbol{\partial h}}{\boldsymbol{\partial b}}\right]$ It's is well known that the good convergence of the NR method is closely linked to the estimation of this tensor. Thus, we proposed a method to provide an accurate approximation of this term.

As described in II, all the constitutive quantities of the Loss Surface model are expressed with analytical functions. So, an exact computation of the scalar incremental permeability is possible as presented in (11)

$$\frac{\partial h}{\partial b} = \frac{\partial h_{anhys}}{\partial b} + \frac{\partial h_{comp}}{\partial b} \tag{11}$$

Then the derivative terms are applied to the projection system to obtain the differential reluctivity tensor as follows in (12)

$$\begin{aligned} \left[\frac{\boldsymbol{\partial h_{anhys}}}{\boldsymbol{\partial b}}\right] &= \frac{\partial h_{anhys}(\|\boldsymbol{b}\|)}{\partial b} \cdot \frac{\boldsymbol{b} \otimes \boldsymbol{b}}{\|\boldsymbol{b}\|^2} \\ \left[\frac{\boldsymbol{\partial h_{comp}}}{\boldsymbol{\partial b}}\right] &= \sum_{i=1}^{N} \omega_i \frac{\partial h_{comp}(\boldsymbol{b} \cdot \boldsymbol{e_{\phi,i}})}{\partial b} \cdot \boldsymbol{e_{\phi,i}} \otimes \boldsymbol{e_{\phi,i}} \end{aligned} \tag{12}$$

The transient problem is solved using a backward Euler scheme, where the nonlinear iterations are initialized using the solution from the previous time step.

V. VALIDATION AND RESULTS

To validate the vector extension of the LS model and its implementation in a FEM code, the numerical procedure was applied to the TEAM problem 32 shown in Fig 4 which is a test problem dedicated to vector hysteresis simulation [10]. The three-limbed transformer with a ferromagnetic core is made from a stack of five 0.48 mm thick non-grain oriented steel laminations. Two windings of 90 turns are placed on the external limbs and can be both connected together or supplied by two independant controlled voltage sources. Since our code does not incorporate external circuit connection, we imposed the experimental current waveforms provided by Bottauscio et al [15] assuming the current density is uniform in the coils.

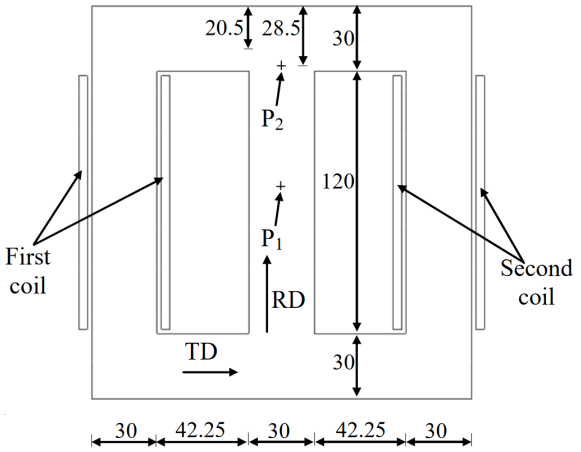

Fig. 4: Geometry of the TEAM problem 32 and position of sensor 1 and 2

For comparison, the same device was modeled in Altair Flux™ with its transient magnetic FEM application. In Flux™, the same mesh was employed and the hysteretic behaviour of the core was described by its built-in vector Preisach model [10]. For the FE problem, the geometry is meshed with 3000 first order triangular elements. Two periods with 200 time steps per period have been simulated.

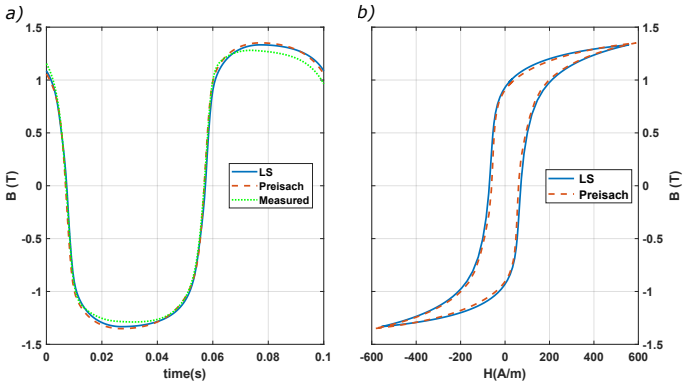

Fig. 5: Case 1: a) Computed and measured flux densities at sensor P1 b) Hysteresis cycles

In the test cases 1 and 2, the windings are connected in series and thus fed with the same sinusoidal current at 10 Hz. In case 2, a distorted signal with a 5th harmonics in phase with the fundamental is tested. The uniaxial flux densities generated in the central limb by both models are compared with the experimental results in Fig. 5.a) and 6.a). The simulations results agree well in case 1, but both models tend to overestimate the decrease due to the harmonics in case 2 as shown in Fig. 6.a). In Fig. 5.b) and 6.b) the hysteresis cycles obtained for both cases are plotted. In case 1, there is agreement between the proposed model and Preisach model. However, the LS vector model allows for a better

representation of minor cycles generated by the fifth harmonics as it can be seen in Fig 6.b).

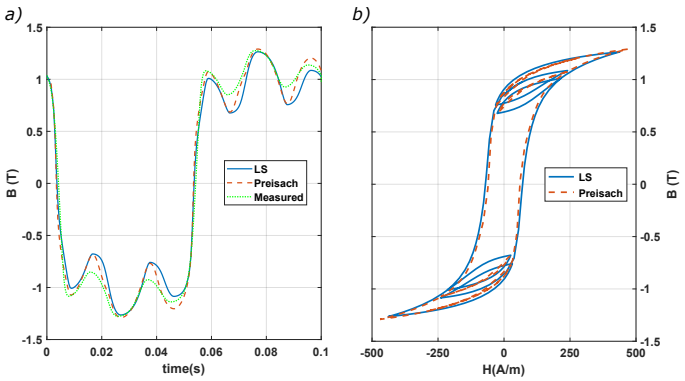

Fig. 6: Case 2: a) Computed and measured flux densities at sensor P1 b) Hysteresis cycles

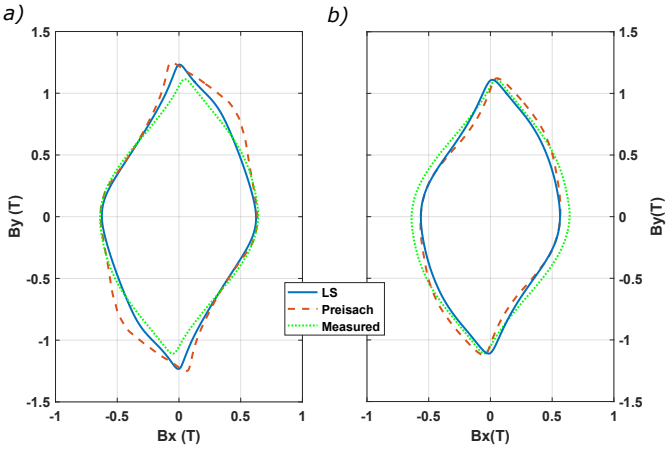

Fig. 7: Case 3: a) Computed and measured b-loci at sensor P2 RD b) Computed and measured b-loci at sensor P2 TD

In the test case 3, the left and right 90 turns windings are fed by two 10 Hz sinusoidal currents, out of phase by 90° producing rotating field at the T-joint of the transformer. For this case, we perform two identifications for each model using the material data provided in [15]: the first one in the rolling direction (RD) and the second one in the transverse direction (TD).

The results for sensor P2 set at the T-joint are compared with the experimental data in Fig. 7.a) and 7.b). A good concordance between the proposed vector extension of the LS model and the Preisach model is observed for both identification with a short better fitting of the LS results with experiment. As specified in Fig. 4, RD (y axis) and TD (x axis) are clearly separated in the transformer. To evaluate the impact of our isotropic approximation we compare the results obtained for each identification. For the RD identification, models overestimate the induction near the RD axis and fit well along TD axis. This can be explained by the fact that for the same imposed exciting current, the models provide higher flux densities in horizontal limbs than in real device, TD being harder magnetization direction than RD. In the same way for the TD identification, models tend to underestimate induction close to the x axis.

For these three test cases, the NR method needs in average less than 10 iterations to converge. This point could be improved by the introduction of a optimized relaxation factor.

VI. Conclusion

In this work, a first implementation of the vector extension of the Loss Surface hysteresis model in 2D finite element analysis is presented and detailed. The Mayergoyz's method has been employed to generalize the scalar model. The proposed model shows good agreement on both uniaxial and rotating excitation compared to the classical Preisach and to measurements. It provides an accurate estimation of the differential reluctivity tensor allowing a good convergence of Newton-Raphson method. An improvement of the numerical performances could be considered by using a method to find an optimal relaxation factor. As mentioned at the beginning, the next step is the generalization of the global LS model including dynamic contribution.

References

[1] G. Bertotti,"Hysteresis in magnetism for physicists, materials scientists, and engineers", Gulf Professional Publishing, 1998

[2] A. Frias, A. Kedous-Lebouc, C. Chillet, L. Albert, L. Calegari, and O. Messal, "Loss minimization of an electrical vehicle machine considering its control and iron losses," IEEE Trans. Magn., vol. 52, no. 5, pp. 1–4, May 2016

[3] D. C. Jiles and D. L. Atherton, "Theory of ferromagnetic hysteresis," J. Magn. Magn. Mater., vol. 61, no. 1-2, pp. 48–60, 1986.

[4] I. D. "Mayergoyz, Mathematical Models of Hysteresis" .NewYork, NY, USA: Springer Verlag, 1991.

[5] A. J. Bergqvist, "A simple vector generalization of the Jiles-Atherton model of hysteresis," IEEE Trans. Magn., vol. 32, no. 5, pp. 4213–4215, 1996.

[6] I. D. Mayergoyz, "Vector Preisach hysteresis models (invited)", Journal of Applied Physics, vol. 63, pp. 2995-3000, April. 1988

[7] E. Dlala, J. Saitz, and A. Arkkio, "Inverted and forward Preisach models for numerical analysis of electromagnetic field problems," IEEE Trans. Magn., vol. 42, no. 8, pp. 1963–1973, Aug. 2006.

[8] J. V. Leite, N. Sadowski, P. Kuo-Peng, N. J. Batistela, J. P. A. Bastos, and A. A. de Espíndola, "Inverse Jiles-Atherton vector hysteresis model," IEEE Trans. Magn., vol. 40, no. 4, pp. 1769–1775, 2004.

[9] C. Guerin, K. Jacques, R. V. Sabariego, P. Dular, C. Geuzaine, and J. Gyselinck, "Using a Jiles–Atherton vector hysteresis model for isotropic magnetic materials with the finite element method, Newton-Raphson method, and relaxation procedure," Int. J. Numer. Model., Electron. Netw., Devices Fields, vol. 30, no. 5, p. e2189, 2016

[10] M. Tousignant, F. Sirois, G. Meunier, and C. Guerin, "Incorporation of a vector Preisach–Mayergoyz hysteresis model in 3-D finite element analysis," IEEE Trans. Magn., vol. 55, no. 6, pp. 1–4, Jun. 2019.

[11] O. Messal, A-T Vo, M. Fassenet, V. Préault, C. Espanet, A. Kedous-Lebouc, "Advanced approach for static part of loss-surface iron loss model, Journal of Magnetism and Magnetic Materials," Volume 502, 2020

[12] A-T Vo , M. Fassenet, A. Kedous-Lebouc, "New formulation of Loss-Surface Model for accurate iron loss modeling at extreme flux density and flux variation: Experimental analysis and test on a high-speed PMSM,"Journal of Magnetism and Magnetic Materials, Volume 563, 2022

[13] C. Appino, M. Khan, O. de la Barrière, C. Ragusa, and F. Fiorillo,"Alternating and rotational losses up to magnetic saturation in non-oriented steel sheets," IEEE Trans. Magn., vol. 52, no. 5, May 2016.

[14] T. Matsuo,"Rotational Saturation Properties of Isotropic Vector Hysteresis Models Using Vectorized Stop and Play Hysterons" IEEE Trans. Magn., vol. 44, no.15, Nov 2008.

[15] O. Bottauscio, M. Chiampi, C. Ragusa, L. Rege, and M. Repetto, "A test case for validation of magnetic field analysis with vector hysteresis," IEEE Trans. Magn., vol. 38, no. 2, pp. 893–896, Mar. 2002.